Reliable Computing **9:** 359–372, 2003.

Some Computer Assisted Proofs for Solutions of the Heat Convection Problems

MITSUHIRO T. NAKAO
Faculty of Mathematics, Kyushu University, Fukuoka 812–8581, Japan,
e-mail: mtnakao@math.kyushu-u.ac.jp

YOSHITAKA WATANABE
Computing and Communications Center, Kyushu University, Fukuoka 812–8581, Japan,
e-mail: watanabe@cc.kyushu-u.ac.jp

NOBITO YAMAMOTO
Department of Computer Science and Information Mathematics, The University of Electro-Communications, Chofu 182–8585, Japan, e-mail: yamamoto@masuo.im.uec.ac.jp

and

TAKAAKI NISHIDA
Graduate School of Science, Kyoto University, Kyoto 606–8502, Japan,
e-mail: a50258@sakura.kudpc.kyoto-u.ac.jp

(Received: 1 July 2002; accepted: 28 January 2003)

Abstract. This is a continuation of our previous results (Y. Watanabe, N. Yamamoto, T. Nakao, and T. Nishida, "A Numerical Verification of Nontrivial Solutions for the Heat Convection Problem," to appear in the *Journal of Mathematical Fluid Mechanics*). In that work, the authors considered two-dimensional Rayleigh-Bénard convection and proposed an approach to prove existence of steady-state solutions based on an infinite dimensional fixed-point theorem using a Newton-like operator with spectral approximation and constructive error estimates. We numerically verified several exact non-trivial solutions which correspond to solutions bifurcating from the trivial solution. This paper shows more detailed results of verification for given Prandtl and Rayleigh numbers. In particular, we found a new and interesting solution branch which was not obtained in the previous study, and it should enable us to present important information to clarify the global bifurcation structure. All numerical examples discussed are take into account of the effects of rounding errors in the floating point computations.

1. The Rayleigh-Bénard Problems

We consider a plane horizontal layer (see Figure 1) of an incompressible viscous fluid heated from below. At the lower boundary $z = 0$ the layer of fluid is maintained at temperature $T + \delta T$, and the temperature of the upper boundary ($z = h$) is T.

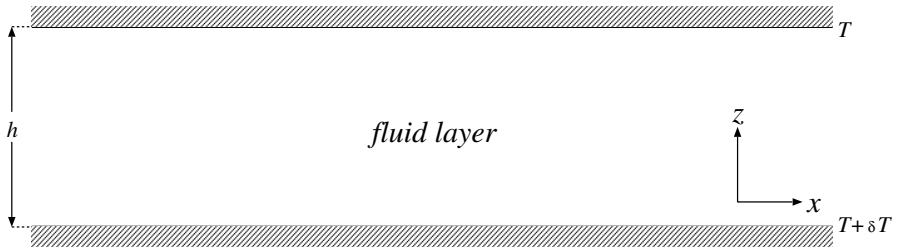

Figure 1. Fluid layer model.

As is well known, assuming the velocity vanishes in the y-direction, the two-dimensional (x-z) heat convection model can be described as the following Oberbeck-Boussinesq approximations [1], [3]:

$$\begin{cases} u_t + uu_x + wu_z = -p_x / \rho_0 + \nu\Delta u, \\ w_t + uw_x + ww_z = -(p_z + g\rho) / \rho_0 + \nu\Delta w, \\ u_x + w_z = 0, \\ \theta_t + u\theta_x + w\theta_z = \kappa\Delta\theta. \end{cases} \tag{1.1}$$

Here,

$u,\ w$: velocity in x and z, respectively,
p : pressure,
θ : temperature,
ρ : fluid density,
ρ_0 : density at temperature $T + \delta T$,
ν : kinematic viscosity,
g : gravitational acceleration,
κ : coefficient of thermal diffusivity,
$*_\xi := \partial / \partial\xi \quad (\xi = x, z, t)$,
$\Delta := \partial^2 / \partial x^2 + \partial^2 / \partial z^2$,

and ρ is assumed to be represented by

$$\rho - \rho_0 = -\rho_0\alpha(\theta - T - \delta T),$$

where α is the coefficient of thermal expansion.

The Oberbeck-Boussinesq equations (1.1) have the following stationary solution:

$$u^* = 0, \quad w^* = 0, \quad \theta^* = T + \delta T - \frac{\delta T}{h}z, \quad p^* = p_0 - g\rho_0\left(z + \frac{\alpha\delta T}{2h}z^2\right),$$

where p_0 is a constant. By setting

$$\hat{u} := u, \qquad \hat{w} := w, \qquad \hat{\theta} := \theta^* - \theta, \qquad \hat{p} := p^* - p,$$

we obtain the transformed equations:

$$\begin{cases} \hat{u}_t + \hat{u}\hat{u}_x + \hat{w}\hat{u}_z = \hat{p}_x / \rho_0 + \nu\Delta\hat{u}, \\ \hat{w}_t + \hat{u}\hat{w}_x + \hat{w}\hat{w}_z = \hat{p}_z / \rho_0 - g\alpha\hat{\theta} + \nu\Delta\hat{w}, \\ \hat{u}_x + \hat{w}_z = 0, \\ \hat{\theta}_t + \delta T\hat{w} / h + \hat{u}\hat{\theta}_x + \hat{w}\hat{\theta}_z = \kappa\Delta\hat{\theta}. \end{cases} \tag{1.2}$$

By further transforming to dimensionless variables:

$$t \to \kappa t, \qquad u \to \hat{u} / \kappa, \qquad w \to \hat{w} / \kappa, \qquad \theta \to \hat{\theta} h / \delta T, \qquad p \to \hat{p} / (\rho_0 \kappa^2)$$

of (1.2), we have the dimensionless equations:

$$\begin{cases} u_t + uu_x + wu_z = p_x + \mathcal{P}\Delta u, \\ w_t + uw_x + ww_z = p_z - \mathcal{P}\mathcal{R}\,\theta + \mathcal{P}\Delta w, \\ u_x + w_z = 0, \\ \theta_t + w + u\theta_x + w\theta_z = \Delta\theta. \end{cases} \tag{1.3}$$

Here

$$\mathcal{R} := \frac{\delta T \alpha g}{\kappa \nu h} \qquad \text{Rayleigh number}$$

and

$$\mathcal{P} := \frac{\nu}{\kappa} \qquad \text{Prandtl number.}$$

2. Fixed-Point Formulation of Problem

In this section, we describe the problem as a fixed point equation of a compact map on the appropriate function space. Since we only consider the *steady-state solutions*, u_t, w_t, and θ_t vanish in (1.3). Also assume that all fluid motion is confined to the rectangular region $\Omega := \{0 < x < 2\pi/a,\ 0 < z < \pi\}$ for a given wave number $a > 0$.

Let us impose a periodic boundary condition (period $2\pi / a$) in the horizontal direction, stress-free boundary conditions ($u_z = w = 0$) for the velocity field and Dirichlet boundary conditions ($\theta = 0$) for the temperature field on the surfaces $z = 0, \pi$, respectively.

Furthermore, we assume the following evenness and oddness conditions:

$$u(x, z) = -u(-x, z), \qquad w(x, z) = w(-x, z), \qquad \theta(x, z) = \theta(-x, z).$$

We use the stream function Ψ satisfying

$$u = -\Psi_z, \qquad w = \Psi_x$$

so that $u_x + w_z = 0$. By some simple calculations in (1.3) after setting $\Theta := \sqrt{\mathcal{PR}}\theta$, we obtain

$$\begin{cases} \mathcal{P}\Delta^2\Psi &= \sqrt{\mathcal{PR}}\,\Theta_x - \Psi_z\Delta\Psi_x + \Psi_x\Delta\Psi_z, \\ -\Delta\Theta &= -\sqrt{\mathcal{PR}}\,\Psi_x + \Psi_z\Theta_x - \Psi_x\Theta_z. \end{cases} \tag{2.1}$$

From the boundary conditions, the functions Ψ and Θ can be assumed to have the following representations:

$$\begin{aligned} \Psi &= \sum_{m=1}^{\infty}\sum_{n=1}^{\infty} A_{mn}\sin(amx)\sin(nz), \\ \Theta &= \sum_{m=0}^{\infty}\sum_{n=1}^{\infty} B_{mn}\cos(amx)\sin(nz). \end{aligned} \tag{2.2}$$

We now define the following function spaces for integers $k \geq 0$:

$$\begin{aligned} X^k := \Bigg\{ &\Psi = \sum_{m=1}^{\infty}\sum_{n=1}^{\infty} A_{mn}\sin(amx)\sin(nz) \mid A_{mn} \in \mathbf{R}, \\ &\sum_{m=1}^{\infty}\sum_{n=1}^{\infty} \left((am)^{2k} + n^{2k}\right) A_{mn}^2 < \infty \Bigg\}, \\ Y^k := \Bigg\{ &\Theta = \sum_{m=0}^{\infty}\sum_{n=1}^{\infty} B_{mn}\cos(amx)\sin(nz) \mid B_{mn} \in \mathbf{R}, \\ &\sum_{m=0}^{\infty}\sum_{n=1}^{\infty} \left((am)^{2k} + n^{2k}\right) B_{mn}^2 < \infty \Bigg\}. \end{aligned}$$

To get our enclosure of the exact solutions for problem (2.1), we need some appropriate finite dimensional subspaces. For $M_1, N_1, M_2 \geq 1$ and $N_2 \geq 0$, we set $N := (M_1, N_1, M_2, N_2)$ and define the finite dimensional approximate subspaces by

$$\begin{aligned} S_N^{(1)} &= \left\{ \Psi_N = \sum_{m=1}^{M_1}\sum_{n=1}^{N_1} \hat{A}_{mn}\sin(amx)\sin(nz) \mid \hat{A}_{mn} \in \mathbf{R} \right\}, \\ S_N^{(2)} &= \left\{ \Theta_N = \sum_{m=0}^{M_2}\sum_{n=1}^{N_2} \hat{B}_{mn}\cos(amx)\sin(nz) \mid \hat{B}_{mn} \in \mathbf{R} \right\}, \\ S_N &= S_N^{(1)} \times S_N^{(2)}. \end{aligned}$$

Denote an approximate solution of (2.1) by $\hat{u}_N := (\hat{\Psi}_N, \hat{\Theta}_N) \in S_N$.

We now set

$$\begin{cases} f_1(\Psi,\Theta) := \sqrt{\mathcal{PR}}\,\Theta_x - \Psi_z\Delta\Psi_x + \Psi_x\Delta\Psi_z, \\ f_2(\Psi,\Theta) := -\sqrt{\mathcal{PR}}\,\Psi_x + \Psi_z\Theta_x - \Psi_x\Theta_z, \end{cases}$$

where

$$\Psi = \hat{\Psi}_N + w^{(1)}, \qquad \Theta = \hat{\Theta}_N + w^{(2)}.$$

Then (2.1) is rewritten as the problem with respect to $(w^{(1)}, w^{(2)}) \in X^4 \times Y^2$ satisfying

$$\begin{cases} \mathcal{P}\Delta^2 w^{(1)} = f_1(\hat{\Psi}_N + w^{(1)},\, \hat{\Theta}_N + w^{(2)}) - \mathcal{P}\Delta^2\hat{\Psi}_N, \\ -\Delta w^{(2)} = f_2(\hat{\Psi}_N + w^{(1)},\, \hat{\Theta}_N + w^{(2)}) + \Delta\hat{\Theta}_N, \end{cases} \tag{2.3}$$

which is the so-called a residual equation. Setting

$$\begin{aligned} w &= (w^{(1)}, w^{(2)}), \\ h_1(w) &= f_1(\hat{\Psi}_N + w^{(1)},\, \hat{\Theta}_N + w^{(2)}) - \mathcal{P}\Delta^2\hat{\Psi}_N, \\ h_2(w) &= f_2(\hat{\Psi}_N + w^{(1)},\, \hat{\Theta}_N + w^{(2)}) + \Delta\hat{\Theta}_N, \\ h(w) &= \big(h_1(w), h_2(w)\big), \end{aligned}$$

by virtue of the Sobolev embedding theorem and the definition of f_1 and f_2, h is a bounded continuous map from $X^3 \times Y^1$ to $X^0 \times Y^0$. Moreover, it is easily shown that for all $(g_1, g_2) \in X^0 \times Y^0$, the linear problem:

$$\begin{cases} \Delta^2\bar{\Psi} = g_1, \\ -\Delta\bar{\Theta} = g_2 \end{cases} \tag{2.4}$$

has a unique solution $(\bar{\Psi}, \bar{\Theta}) \in X^4 \times Y^2$. We denote this mapping by $\bar{\Psi} = (\Delta^2)^{-1}g_1$ and $\bar{\Theta} = (-\Delta)^{-1}g_2$, so the operator

$$\mathcal{K} := \big(\mathcal{P}^{-1}(\Delta^2)^{-1}, (-\Delta)^{-1}\big) : X^0 \times Y^0 \to X^3 \times Y^1$$

is a compact map (because of the compactness of the imbedding $X^4 \hookrightarrow X^3$ and $Y^2 \hookrightarrow Y^1$ and the boundedness of $(\Delta^2)^{-1} : X^0 \to X^4$, $(-\Delta)^{-1} : Y^0 \to Y^2$). Thus, (2.3) is rewritten as a fixed-point equation:

$$w = Fw \tag{2.5}$$

for the compact operator $F := \mathcal{K} \circ h$ on $X^3 \times Y^1$. Therefore, by the Schauder fixed-point theorem, if we find a nonempty, closed, bounded and convex set $W \subset X^3 \times Y^1$, satisfying

$$FW \subset W \tag{2.6}$$

then there exists a solution of (2.5) in W. The set W in (2.6) is called a *candidate set* of solutions.

3. Constructive Error Estimates and Computable Verification Condition

To obtain the set W satisfying (2.6), we need a projection into S_N and its constructive a priori error estimates.

For $\Psi \in X^3$ and $\Theta \in Y^1$, let us define projections $P_N^{(1)}\Psi \in S_N^{(1)}$ and $P_N^{(2)}\Theta \in S_N^{(2)}$ by

$$\begin{cases} \left(\Delta(P_N^{(1)}\Psi - \Psi),\, \Delta v_N^{(1)}\right)_{L^2} = 0 & \forall v_N^{(1)} \in S_N^{(1)}, \\ \left(\nabla(P_N^{(2)}\Theta - \Theta),\, \nabla v_N^{(2)}\right)_{L^2} = 0 & \forall v_N^{(2)} \in S_N^{(2)}. \end{cases} \tag{3.1}$$

Now we denote the L^2-inner product and the L^2-norm on Ω by $(\cdot,\,\cdot)_{L^2}$ and $\|\cdot\|_{L^2}$, respectively, and also define the H_0^1-norm: $\|\nabla u\|_{L^2}$ and the H^k-norm: $\|u\|_{H^k}$ on Ω by $\|\nabla u\|_{L^2}^2 = \|u_x\|_{L^2}^2 + \|u_z\|_{L^2}^2$ and $\|u\|_{H^k}^2 = \sum_{i,j\in\mathbf{N},\ i+j\le k} \|\partial^{i+j}u \,/\, \partial^i x \partial^j z\|_{L^2}^2$, respectively. The norms in X^k and Y^k are defined naturally by the H^k-norm on Ω.

For each $(g_1, g_2) \in X^0 \times Y^0$, let $(\psi, \theta) \in X^4 \times Y^2$ be the solution of (2.4), and let $(P_N^{(1)}\psi, P_N^{(2)}\theta) \in S_N$ be finite dimensional approximations defined by (3.1). Then, we have constructive a priori error estimates of the form:

$$\|\psi - P_N^{(1)}\psi\|_{H^k} \le C_{1,k}\|g_1\|_{L^2} \quad \text{and} \quad \|\theta - P_N^{(2)}\theta\|_{H^k} \le C_{2,k}\|g_2\|_{L^2}. \tag{3.2}$$

Here the $C_{i,k}$ are numerically estimated, e.g., such as

$$C_{1,1} \le \max\left\{\frac{1}{(a^2 + (N_1+1)^2)^2},\ \frac{1}{(a^2(M_1+1)^2+1)^2}\right\};$$

see [9] for details.

We now reformulate the verification condition (2.6) by applying the Newton-like method for nonlinear elliptic problems proposed by the author [6], [7]. Defining the projection from $X^3 \times Y^1$ into S_N by

$$P_N = (P_N^{(1)}, P_N^{(2)}),$$

the fixed-point problem $w = Fw$ can be decomposed into finite dimensional and infinite dimensional parts as follows:

$$\begin{cases} P_N w = P_N F w, \\ (I - P_N)w = (I - P_N)Fw, \end{cases} \tag{3.3}$$

where I is the identity map on $X^3 \times Y^1$. We assume that the restriction of the operator $I - P_N\mathcal{K}f'(\hat{u}_N) : X^3 \times Y^1 \longrightarrow S_N$ to S_N has an inverse

$$[I - P_N\mathcal{K}f'(\hat{u}_N)]_N^{-1} : S_N \longrightarrow S_N, \tag{3.4}$$

where $f'(\hat{u}_N)$ denotes the Fréchet derivative of $f := (f_1, f_2)$ at the approximate solution $\hat{u}_N$ which coincides with $h'(0)$. Then, we define the operator $\mathcal{N}_N : X^3 \times Y^1 \longrightarrow S_N$ by

$$\mathcal{N}_N w = P_N w - [I - P_N\mathcal{K}f'(\hat{u}_N)]_N^{-1} P_N(I - F)w$$

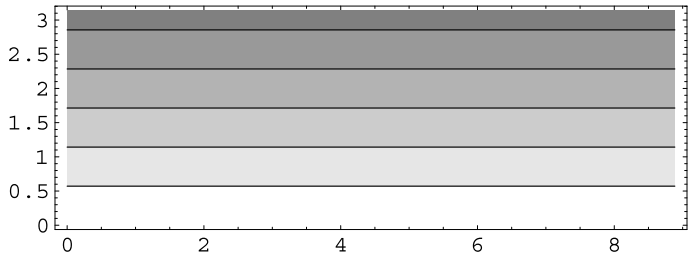

Figure 2. The isotherm of the temperature: stationary solution.

and the compact map $T : X^3 \times Y^1 \longrightarrow X^3 \times Y^1$ by

$$Tw = \mathcal{N}_N w + (I - P_N)Fw.$$

Since $w = Fw \Leftrightarrow w = Tw$, we have a computable verification condition of the form:

$$TW \subset W, \tag{3.5}$$

where, usually, the candidate set W is taken to be as

$$W = W_N \oplus W_*$$

with $W_N \subset S_N$ and $W_* \subset {S_N}^{\perp}$. Therefore, (3.5) is equivalently rewritten as

$$\begin{cases} \mathcal{N}_N W \subset W_N, \\ (I - P_N)FW \subset W_*. \end{cases} \tag{3.6}$$

We omit the detailed verification procedures based upon this criterion (see, e.g., [6], [7], [9], etc.).

4. Numerical Results

We have successfully verified several kinds of bifurcating solutions which actually exist on the different bifurcation branches. With results rather complicated bifurcation structure can be clarified for our problem, even though only solutions on relatively simple branches were enclosed in [9].

4.1. The Trivial Solution

It is clear that the problem (2.1) has a trivial solution $\Psi = \Theta = 0$ for all $\mathcal{P}$ and $\mathcal{R}$. Figure 2 shows the isotherm of the temperature $T + \delta T - \frac{\delta T}{h} z$ when $T = 0$ and $\delta T = 5$.

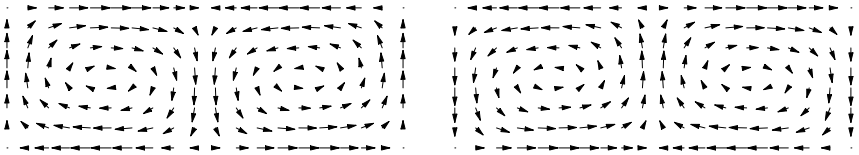

Figure 3. The velocity field of the first bifurcated solution.

It is known that for small $\mathcal{R}$ the fluid conducts heat diffusively, and at a critial point $\mathcal{R}_C$, heat is transported through the fluid by convection. It has been shown by Joseph [4] that (1.3) has a unique trivial solution for $\mathcal{R} < \mathcal{R}_C$. However, the global structure of bifurcated solutions after the critical Rayleigh point $\mathcal{R}_C$ has not been known theoretically.

4.2. First and Second Bifurcated Solutions from the Trivial Solution

In our preceding paper [9], we already verified for several nontrivial solutions corresponding to primary and secondary bifurcating solution branches. Namely, for the case that $a = 1/\sqrt{2}$ and $\mathcal{P} = 10$, the first solution branch appears after the critical Rayleigh number $\mathcal{R}_C = 6.75$.

We obtained two non-trivial approximate solutions for various Rayleigh numbers $\mathcal{R}$ of the form:

$$\hat{\Psi}_N = \sum_{m=1}^{M_1} \sum_{n=1}^{N_1} \hat{A}_{mn} \sin(amx) \sin(nz),$$
$$\hat{\Theta}_N = \sum_{m=0}^{M_2} \sum_{n=1}^{N_2} \hat{B}_{mn} \cos(amx) \sin(nz)$$

for some M_1, M_2, N_1, and N_2 by the Fourier-Galerkin method combined with Newton-Raphson iteration. Figure 3 shows the velocity field $(-(\hat{\Psi}_N)_z, (\hat{\Psi}_N)_x)$ at $\mathcal{R} = 50$, $\mathcal{P} = 10$, $M_1 = N_1 = M_2 = N_2 = 10$, respectively. We illustrate the particular value of coefficients, under the figures, which has the maximum absolute value in $\{\hat{A}_{mn}\}$ and $\{\hat{B}_{mn}\}$, respectively.

Figure 4 shows the isotherm of the temperature

$$\theta^* = \delta T(1 - z/\pi - \Theta/\sqrt{\mathcal{R}\mathcal{P}}\pi) + T$$

when $T = 0$, $\delta T = 5$.

For Rayleigh numbers greater than

$$\mathcal{R} = \frac{(a^2m^2 + n^2)^3}{a^2m^2} = 13.5 \qquad (m = 2,\ \ n = 1,\ \ a = 1/\sqrt{2}),$$

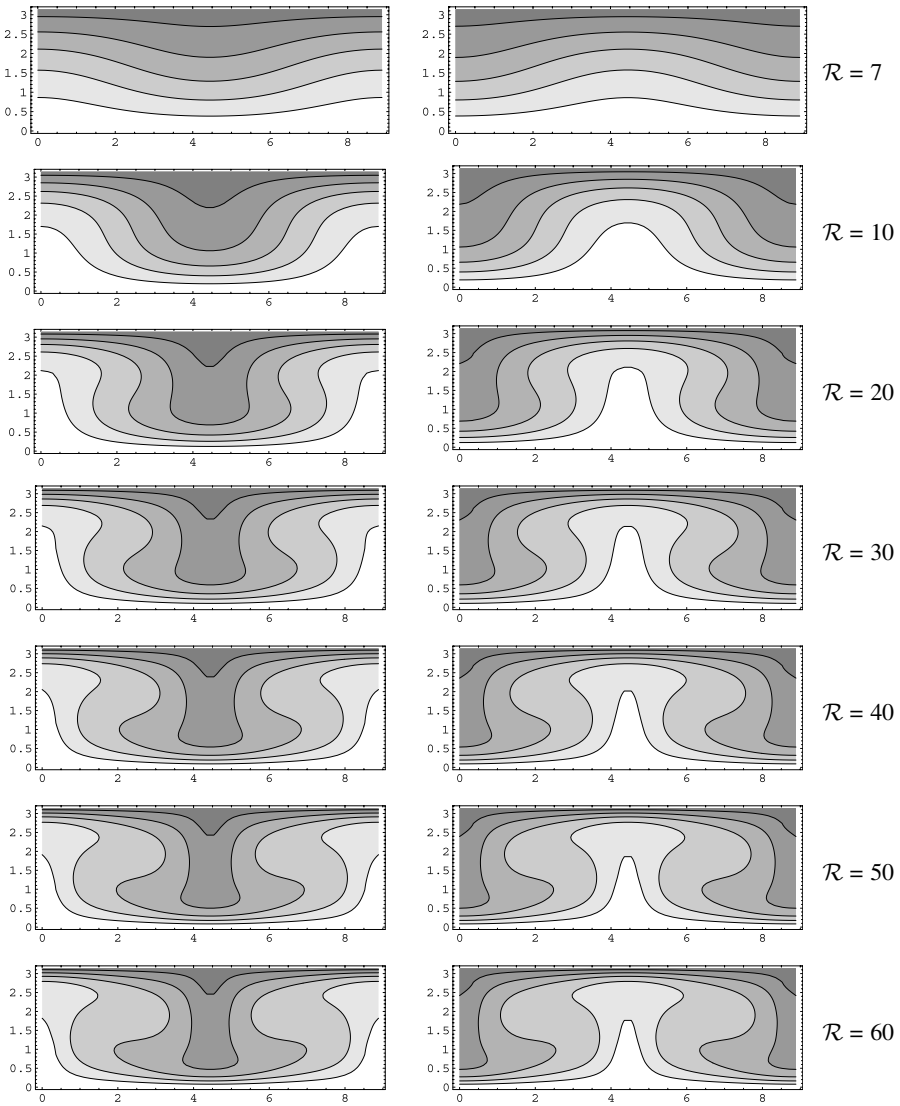

Figure 4. The isotherm of the temperature for the first bifurcated solution.

we obtained two non-trivial approximate solutions which are thought to be secondary bifurcating solutions from the trivial solution. Figure 5 and Figure 6 show the velocity field at $\mathcal{R} = 50$, $\mathcal{P} = 10$, $M_1 = N_1 = M_2 = N_2 = 10$ and the isotherm of the temperature, respectively.

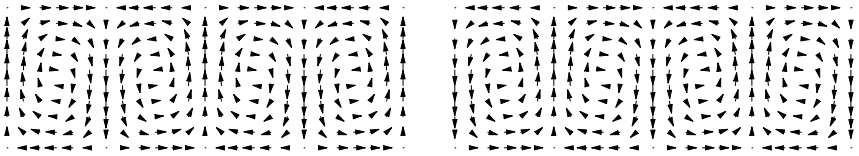

$\hat{A}_{21} \approx -7.026$ $\hat{A}_{21} \approx 7.026$

Figure 5. The velocity field of the secondary bifurcated solution.

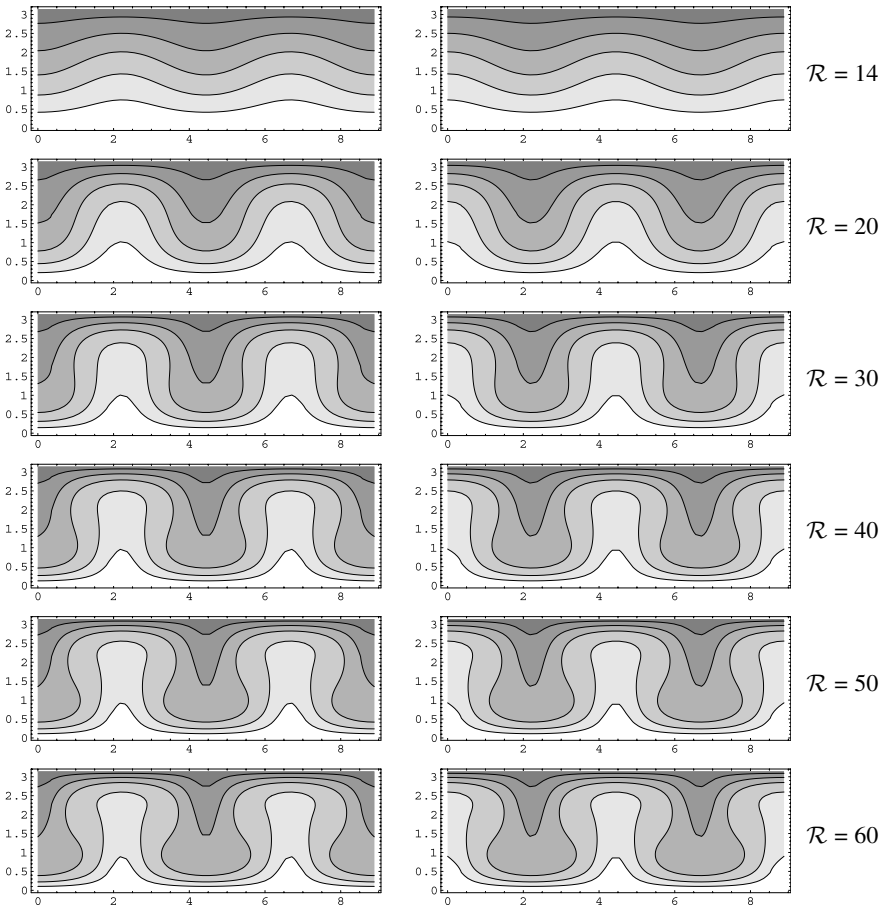

Figure 6. The isotherm of the temperature for the secondary bifurcated solution.

4.3. Third Bifurcated Solutions from the Trivial Solution

For Rayleigh numbers greater than

$$\mathcal{R} = \frac{(a^2m^2 + n^2)^3}{a^2m^2} = 1331 / 36 \qquad (m = 3, n = 1, a = 1 / \sqrt{2}),$$

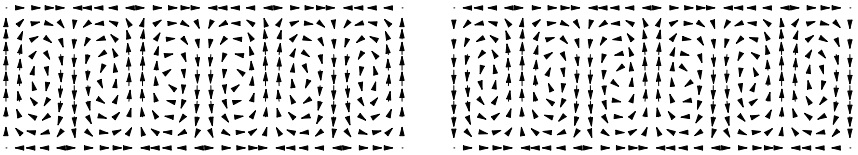

Figure 7. The velocity field of the tertiary bifurcated solution.

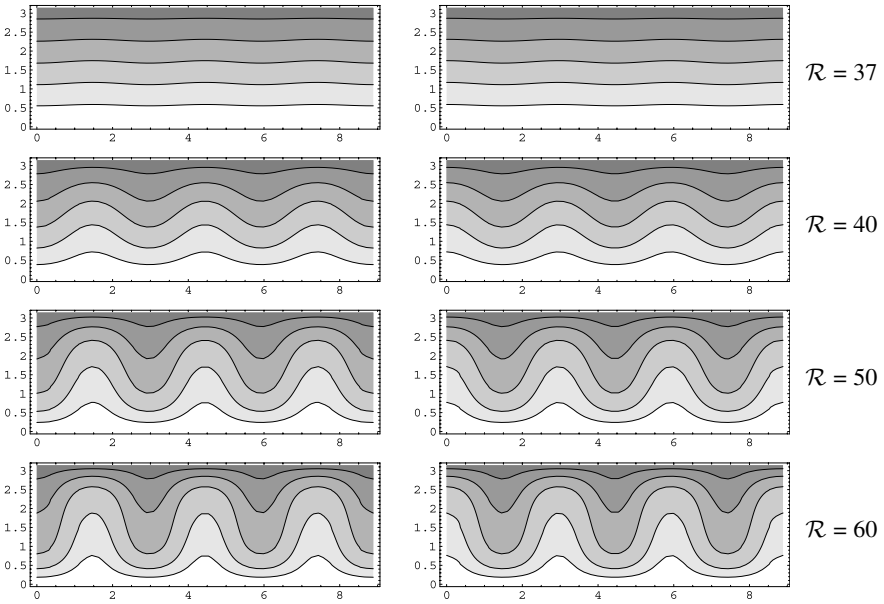

Figure 8. The isotherm of the temperature for the tertiary bifurcated solution.

we obtained two non-trivial approximate solutions which are thought to be tertiary bifurcating solutions from the trivial solution. Figure 7 and Figure 8 show the velocity field at $\mathcal{R} = 50$, $\mathcal{P} = 10$, $M_1 = N_1 = M_2 = N_2 = 10$ and the isotherm of the temperature, respectively.

4.4. Another Non-Trivial Solutions

We also calculated four different non-trivial approximate solutions after $\mathcal{R} = 32.5$. According to those computational results, we expect the existence of another bifurcation curve bifurcating from the secondary bifurcation branch (cf. Figure 11). For example, we observed the phenomena as shown in Figure 9 and Figure 10 when $\mathcal{R} = 50$, $\mathcal{P} = 10$, $M_1 = N_1 = M_2 = N_2 = 10$. Actually we could verify such solution branches.

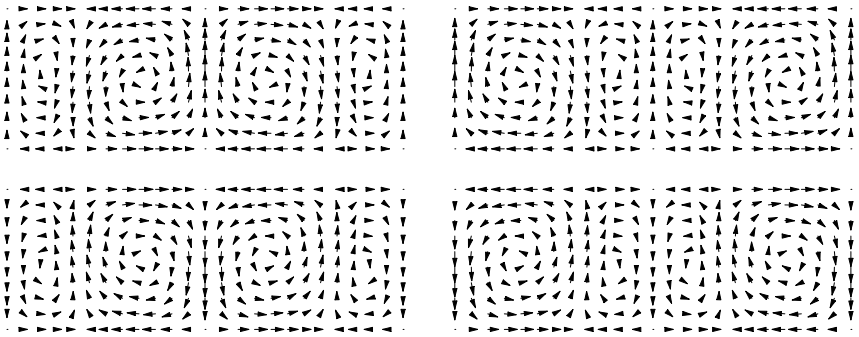

Figure 9. The velocity field of the other non-trivial solutions.

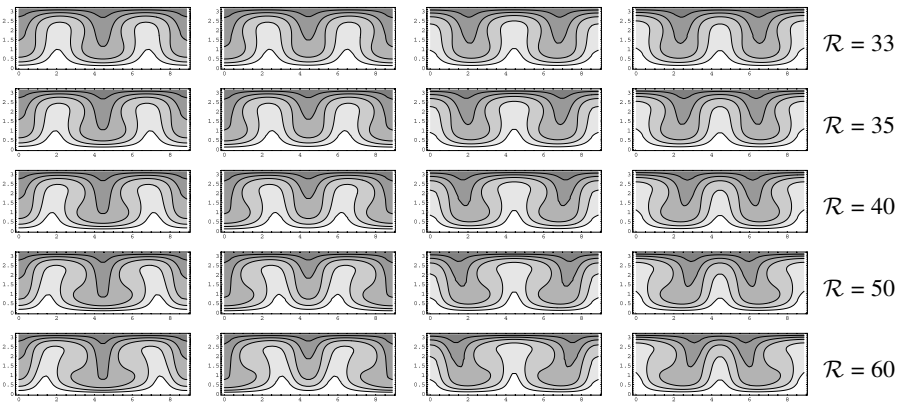

Figure 10. The isotherm of the temperature for the other non-trivial solutions.

4.5. VERIFICATION RESULTS

As a whole, we succeeded in verifying the exact solutions of (2.1) corresponding to the approximate solutions shown in Figure 11. The vertical axis shows the absolute value of the coefficient of the approximate solution: $\hat{\Theta}_N = \sum_{m=0}^{M_2} \sum_{n=1}^{N_2} \hat{B}_{mn} \sin(amx) \sin(nz)$. Each dot implies that the verification procedure resulted in success.

In particular, for the case $\mathcal{R} = 60$, $\mathcal{P} = 10$ with $N := M_1 = M_2 = N_1 = N_2$, we could enclose 10 different solutions whose error bounds are shown in Table 1. In the table, half of the solutions could have been obtained from symmetry properties of the problem. It might also be possible to show pitchfork type bifurcation structure by drawing the diagram appropriately. In Table 1, there exists a solution

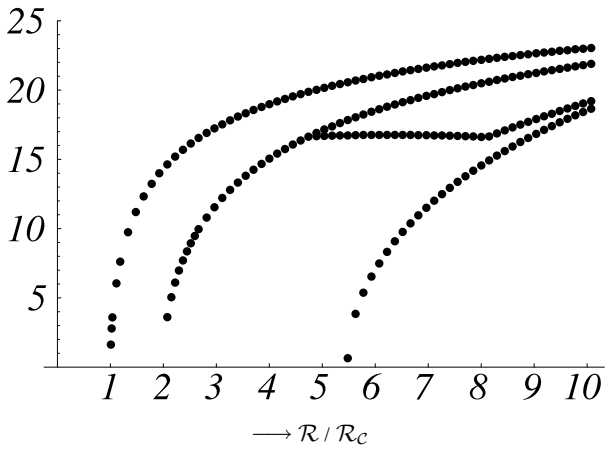

Figure 11. The bifurcation structure.

Table 1. Verification results; $\mathcal{R} = 60$, $\mathcal{P} = 10$.

No.	N	$\|\hat{\Psi}_N\|_{L^2}$	$\|\hat{\Theta}_N\|_{L^2}$	$\|W_N^{(1)}\|_{L^\infty}$	$\|W_N^{(2)}\|_{L^\infty}$	$\|W_*^{(1)}\|_{L^\infty}$	$\|W_*^{(2)}\|_{L^\infty}$
1	45	17.44	34.89	1.40×10^{-9}	3.12×10^{-11}	2.46×10^{-11}	1.26×10^{-7}
2	45	17.44	34.89	1.40×10^{-9}	3.12×10^{-11}	2.46×10^{-11}	1.26×10^{-7}
3	30	8.14	30.57	2.35×10^{-6}	2.56×10^{-8}	7.75×10^{-8}	1.35×10^{-4}
4	30	8.14	30.57	2.35×10^{-6}	2.56×10^{-8}	7.75×10^{-8}	1.35×10^{-4}
5	50	9.62	29.43	9.75×10^{-9}	8.77×10^{-10}	6.96×10^{-11}	5.21×10^{-7}
6	50	9.62	29.43	9.75×10^{-9}	8.77×10^{-10}	6.96×10^{-11}	5.21×10^{-7}
7	50	9.62	29.43	9.75×10^{-9}	8.77×10^{-10}	6.96×10^{-11}	5.21×10^{-7}
8	50	9.62	29.43	9.75×10^{-9}	8.77×10^{-10}	6.96×10^{-11}	5.21×10^{-7}
9	20	2.84	19.49	3.40×10^{-5}	9.56×10^{-7}	1.75×10^{-6}	1.10×10^{-3}
10	20	2.84	19.49	3.40×10^{-5}	9.56×10^{-7}	1.75×10^{-6}	1.10×10^{-3}

$(\Psi, \Theta) \in X^3 \times Y^1$ of (2.1) in:

$$\Psi \in \hat{\Psi}_N + W_N^{(1)} + W_*^{(1)},$$
$$\Theta \in \hat{\Theta}_N + W_N^{(2)} + W_*^{(2)}.$$

Remark 4.1. In Figure 11, each dot shows the corresponding solution is verified in a mathematically rigorous sense. Therefore, it also implies that we have established a computer assisted proof in the analysis of our heat convection problem. However, from our verification results we cannot at present determine whether the verified solutions are really bifurcated or simply isolated solutions. This question should be solved in our future work.

We used the following software for the verified numerical computations: Fortran 90 library `INTLIB_90` coded by Kearfott [5] with DIGITAL Fortran V5.4–1283 on Compaq Alpha Server GS320 (Alpha 21264 731 MHz; Tru64 UNIX V5.1).

The authors are very grateful to Professor Kearfott for his kind implementation and release of this useful software package.

References

1. Chandrasekhar, S.: *Hydrodynamic and Hydromagnetic Stability*, Oxford University Press, 1961.
2. Curry, J. H.: Bounded Solutions of Finite Dimensional Approximations to the Boussinesq Equations, *SIAM J. Math. Anal.* **10** (1979), pp. 71–79.
3. Getling, A. V.: Rayleigh-Bénard Convection: Structures and Dynamics, *Advanced Series in Nonlinear Dynamics* **11**, World Scientific, 1998.
4. Joseph, D. D.: On the Stability of the Boussinesq Equations, *Arch. Rational Mech. Anal.* **20** (1965), pp. 59–71.
5. Kearfott, R. B. and Kreinovich, V.: *Applications of Interval Computations*, Kluwer Academic Publishers, Dordrecht, 1996.
6. Nakao, M. T.: A Numerical Verification Method for the Existence of Weak Solutions for Nonlinear Boundary Value Problems, *J. Math. Anal. Appl.* **164** (1992), pp. 489–507.
7. Nakao, M. T.: Solving Nonlinear Elliptic Problems with Result Verification Using an H^{-1} Type Residual Iteration, *Computing, Suppl.* **9** (1993), pp. 161–173.
8. Rayleigh, J. W. S.: On Convection Currents in a Horizontal Layer of Fluid, When the Higher Temperature Is on the Under Side, *The London, Edinburgh and Dublin Philosophical Magazine and Journal of Science, Ser. 6* **32** (1916), pp. 529–546; and *Scientific Papers* **6** (1920), pp. 432–446.
9. Watanabe, Y., Yamamoto, N., Nakao, M. T., and Nishida, T.: A Numerical Verification of Nontrivial Solutions for the Heat Convection Problem, *Journal of Mathematical Fluid Mechanics*, to appear.